

One-Dimensional Chain of Tetranuclear Manganese Single-Molecule Magnets

Jae Yoo,[†] Wolfgang Wernsdorfer,[‡] En-Che Yang,[†] Motohiro Nakano,[†] Arnold L. Rheingold,[†] and David N. Hendrickson^{*†}

Department of Chemistry and Biochemistry-0358, University of California at San Diego, La Jolla, California 92093-0358, and Laboratoire Louis Néel-CNRS, 25 Avenue des Martyrs, 38042 Grenoble Cedex 9, France

Received December 17, 2004

A one-dimensional chain of interconnected single-molecule magnets (SMMs) is obtained that consists of $[\text{Mn}_4(\text{hmp})_6]^{4+}$ units bridged by chloride ions. Slow magnetization relaxation is evident in the AC susceptibility data and in magnetization hysteresis measurements for $[\text{Mn}_4(\text{hmp})_6\text{Cl}_2]_n(\text{ClO}_4)_{2n}$. The magnetization hysteresis loops for this complex are similar to those for an SMM and show significant coercive field and steps at regular magnetic intervals. Spin-canted antiferromagnetic coupling due to misalignment of easy axes of neighboring Mn_4 units is also observed for this complex.

There is a growing interest in molecules that are nanomagnets.^{1,2} There are three requirements for an individual molecule to function as a single-molecule magnet (SMM): a large spin (S) ground state, negative magnetoanisotropy, and the absence of strong tunnel splitting between different M_s states of an SMM that leads to rapid magnetization tunneling. In comparison to classical nanomagnets, the molecular nature of SMMs facilitates systematic changes in their architecture. This has led for the first time to benchmark observations on the magnetization dynamics of nanomagnets, including such effects as quantum tunneling of magnetization,^{3,4} spin-parity effects,⁵ exchange biasing due to intermolecular magnetic exchange interactions,⁶ and spin–spin cross-relaxation.⁷ The ligands employed to prepare SMMs

have been modified to discover Jahn–Teller isomers⁸ of Mn_{12} complexes, the largest-molecular-weight Mn_{84} SMM,⁹ and the largest-spin ($S = 51/2$) SMM.¹⁰ However, there have been very few reports wherein SMMs have been connected together via bridges to form one-, two-, and three-dimensional arrays.¹¹ In this communication, we report the preparation of a one-dimensional chain of interconnected SMMs.

We recently reported a series of tetramanganese SMMs with the chemical compositions $[\text{Mn}_4(\text{OAc})_2(\text{pdmH})_6]-(\text{ClO}_4)_2$ (**1**),¹² $[\text{Mn}_4(\text{hmp})_6\text{Br}_2(\text{H}_2\text{O})_2]\text{Br}_2 \cdot 4\text{H}_2\text{O}$ (**2**),¹³ $[\text{Mn}_4(\text{hmp})_6(\text{NO}_3)_2(\text{CH}_3\text{CN})_2](\text{ClO}_4)_2 \cdot 2\text{CH}_3\text{CN}$ (**3**), and $[\text{Mn}_4(\text{hmp})_6(\text{NO}_3)_4]$ (**4**).¹⁴ All four complexes contain a $\text{Mn}_2^{\text{III}}\text{Mn}_2^{\text{II}}$ dicubane core, incorporating the monoanionic ligand 2,6-pyridinedimethanol (pdmH^-) or 2-hydroxymethylpyridine (hmp^-) as a bridging ligand. These complexes were determined by high-frequency EPR (HF-EPR) and magnetization versus magnetic field data to have a $S = 9$ ground state. In the present communication, the $[\text{Mn}_4(\text{hmp})_6]^{4+}$ SMM unit is assembled into a one-dimensional magnetic chain. The compound $[\text{Mn}_4(\text{hmp})_6\text{Cl}_2]_n(\text{ClO}_4)_{2n}$ (**5**) was synthesized by reacting MnCl_2 (4 equiv) with n -tetrabutylammonium permanganate (1 equiv) in the presence of hmpH (10 equiv)

* To whom correspondence should be addressed. E-mail: dhendrickson@ucsd.edu.

[†] University of California at San Diego.

[‡] Laboratoire Louis Néel-CNRS.

- (1) Sessoli, R.; Tsai, H.-L.; Schake, A. R.; Wang, S.; Vincent, J. B.; Foltling, K.; Gatteschi, D.; Christou, G.; Hendrickson, D. N. *J. Am. Chem. Soc.* **1993**, *115*, 1804–1806.
- (2) Christou, G.; Gatteschi, D.; Hendrickson, D. N.; Sessoli, R. *MRS Bull.* **2000**, *25*, 66.
- (3) Thomas, L.; Lioni, F.; Ballou, R.; Gatteschi, D.; Sessoli, R.; Barbara, B. *Nature* **1996**, *383*, 145.
- (4) Friedman, J. R.; Sarachik, M. P.; Tejada, J.; Ziolo, R. *J. Appl. Phys.* **1996**, *79*, 6031.
- (5) Wernsdorfer, W.; Bhaduri, S.; Boskovic, C.; Christou, G.; Hendrickson, D. N. *Phys. Rev. B* **2002**, *65*, 180403.
- (6) Wernsdorfer, W.; Aliaga-Alead N.; Hendrickson, D. N.; Christou, G. *Nature* **2002**, *416*, 406.

- (7) Wernsdorfer, W.; Bhaduri, S.; Tiron, R.; Hendrickson, D. N.; Christou, G. *Phys. Rev. Lett.* **2002**, *89*, 197201.
- (8) Aubin, S. M. J.; Sun, Z.; Eppley, H. J.; Rumberger, E. M.; Guzei, I. A.; Foltling, K.; Gantzel, P. K.; Rheingold, A. L.; Christou, G.; Hendrickson, D. N. *Inorg. Chem.* **2001**, *40*, 2127–2146.
- (9) Tasiopoulos, A. J.; Vinslava, A.; Wernsdorfer, W.; Abboud, K. A.; Christou, G. *Angew. Chem., Int. Ed.* **2004**, *43* (16), 2117–2121.
- (10) Murugesu, M.; Habrych, M.; Wernsdorfer, W.; Abboud, K. A.; Christou, G. *J. Am. Chem. Soc.* **2004**, *126* (15), 4766–4767.
- (11) (a) Miyasaka, H.; Nakata, K.; Sugiura, K.-I.; Yamashita, M.; Clerac, R. *Angew. Chem., Int. Ed.* **2004**, *43*, 707–711. (b) Shaikh, N.; Panja, A.; Goswami, S.; Banerjee, P.; Vojtisek, P.; Zhang, Y.-Z.; Su, G.; Gao, S. *Inorg. Chem.* **2004**, *43*, 849–851.
- (12) Yoo, J.; Brechin, E. K.; Yamaguchi, A.; Nakano, M.; Huffman, J. C.; Maniero, A. L.; Brunel, L.; Awaga, K.; Ishimoto, H.; Christou, G.; Hendrickson, D. N. *Inorg. Chem.* **2000**, *39*, 3615.
- (13) Yoo, J.; Yamaguchi, A.; Nakano, M.; Krzystek, J.; Streib, W. E.; Brunel, L.-C.; Ishimoto, H.; Christou, G.; Hendrickson, D. N. *Inorg. Chem.* **2001**, *40*, 4604.
- (14) Yang, E.-C.; Harden, N.; Wernsdorfer, W.; Zakharov, L.; Brechin, E. K.; Rheingold, A. L.; Christou, G.; Hendrickson, D. N. *Polyhedron* **2003**, *22*, 1857–1836.

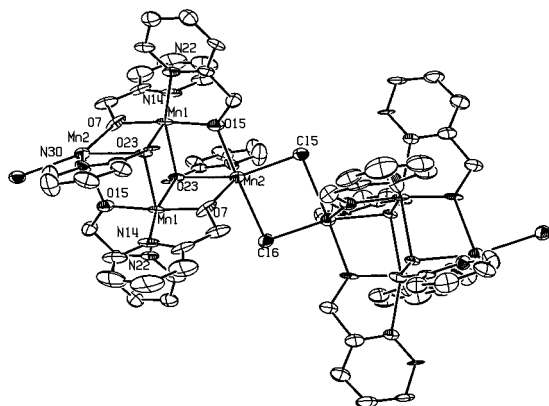


Figure 1. ORTEP representation of the cation of complex **5**.

in ethanol. The resulting red brown solution was then treated with sodium perchlorate (4 equiv), and crystalline product suitable for X-ray crystallography formed after 2 weeks.

The ORTEP plot of two Mn_4 units of the chain $[Mn_4(hmp)_6Cl_2]_n(ClO_4)_{2n}$ (**5**) is shown in Figure 1. Complex **5** crystallizes in the $P1$ space group.¹⁵ The tetranuclear dicubane unit resides on an inversion center, and there are two independent tetranuclear moieties per each unit cell. A notable feature of this complex is that the easy axes of the tetranuclear units are staggered, as indicated by the nonparallel orientation of the Mn^{III} Jahn–Teller axes (ca. 45°) between neighboring tetranuclear units. This nonparallel alignment of easy axes between the neighboring Mn_4 SMMs is the origin of spin canting.

Variable-temperature DC magnetic susceptibility measurements were made for a polycrystalline sample of **5** in a 10 kG magnetic field in the 5–300 K range. The $\chi_M T$ value for complex **5** increases from $14.41 \text{ cm}^3 \text{ mol}^{-1} \text{ K}$ at 300 K to a maximum of $23.4 \text{ cm}^3 \text{ mol}^{-1} \text{ K}$ at 20 K. Below 20 K, it drops to $15.41 \text{ cm}^3 \text{ mol}^{-1} \text{ K}$ at 5 K. The increase in $\chi_M T$ from 300 to 20 K occurs because there are ferromagnetic interactions in each Mn_4 unit to give an $S = 9$ SMM as observed before. Weak exchange interactions between the Mn_4 SMMs as well as zero-field interactions are likely the origin of the decrease in $\chi_M T$ below 20 K.

To determine the spin of the ground state of complex **5**, variable-field magnetization measurements were performed at applied fields of 20–50 kG in the temperature range 2–4 K. For complex **5**, the magnetization saturates at $13.7 N\mu_B$. The variable-field magnetization data were least-squares fit employing a spin Hamiltonian (eq 1) that incorporates a mean-field correction term for intercluster interactions in addition to Zeeman interaction and axial zero-field splitting (DS_z^2).

$$H = \sum_i [D'(S_{iz})^2 + g\mu_B B S_i - 2j'S_i \cdot S_{i+1}] \quad (1)$$

(15) Crystal data: $C_{36}H_{36}Cl_4Mn_4N_6O_{14}$, $a = 11.643(6) \text{ \AA}$, $b = 11.702(6) \text{ \AA}$, $c = 17.890(9) \text{ \AA}$, $\alpha = 72.939(11)^\circ$, $\beta = 74.285(9)^\circ$, $\gamma = 70.911(19)^\circ$, $V = 2160.4 \text{ \AA}^3$, $Z = 2$, formula weight = $1138.27 \text{ g mol}^{-1}$, space group $P1$, $T = -161^\circ \text{ C}$, $\rho_{\text{calc}} = 1.750 \text{ g/cm}^3$, $R = 0.1055$, $R_w = 0.2320$.

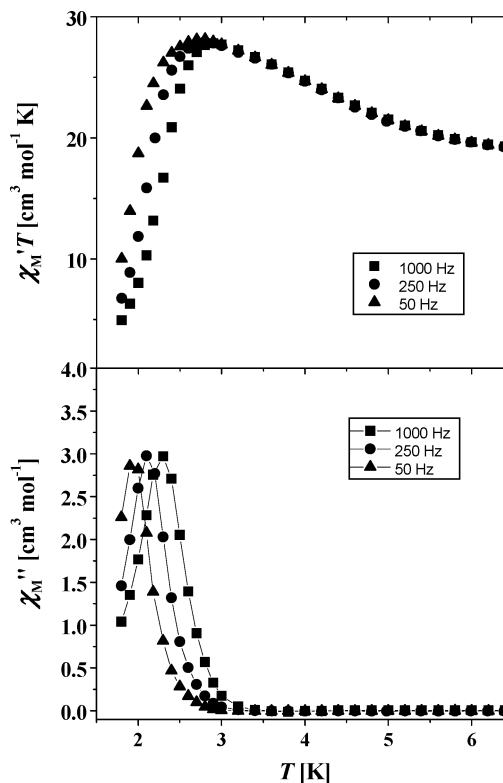


Figure 2. Plot of in-phase $\chi_M' T$ component (top) and out-of-phase χ_M'' component (bottom) of complex **5**.

In this equation, S_i is the resultant spin of each Mn_4 unit ($S = 9$) of the polymer, D' is the zero-field splitting parameter, and j' is the parameter that gauges the intercluster interactions in the chain. Fitting of the data for complex **5** to eq 1 gives the parameter values of $D'/k_B = -0.62 \text{ K}$ and $j'/k_B = -0.077 \text{ K}$.

AC magnetic susceptibility data were also collected under a zero DC field with a 1 G AC field in the 1.8–50 K range. The $\chi_M' T$ value slowly increases from $21 \text{ cm}^3 \text{ mol}^{-1} \text{ K}$ at 50 K to a broad maximum of $24 \text{ cm}^3 \text{ mol}^{-1} \text{ K}$ at 25 K. The $\chi_M' T$ value then gradually decreases below 25 K, but it sharply increases below 7 K and reaches a maximum of $28.8 \text{ cm}^3 \text{ mol}^{-1} \text{ K}$ at 2.9 K. The appearance of the field-dependent spike feature in the $\chi_M' T$ plot at 2.9 K is the result of the canting caused by misalignment of the easy axes of neighboring tetranuclear Mn_4 units. Weak ferromagnetism arises in the case of antiferromagnetically coupled one-dimensional complexes where incomplete cancellation of spins leaves a residual magnetic moment along the chain.

As shown in Figure 2, the AC susceptibility data for the polycrystalline sample of **5** in the temperature range 1.8–3 K exhibit a sharp decrease in the in-phase ($\chi_M' T$) component and the appearance of a strong out-of-phase (χ_M'') peak. Both are frequency-dependent. The presence of a strong frequency dependence in the out-of-phase AC signal indicates that a magnetization relaxation process is occurring in this temperature range. It is likely that this is due to individual $S = 9$ SMM units in the chain.

The AC magnetic susceptibility response was further explored using a DC magnetic field (0–10000 G). Figure 3 shows how the AC data respond to the application of a DC

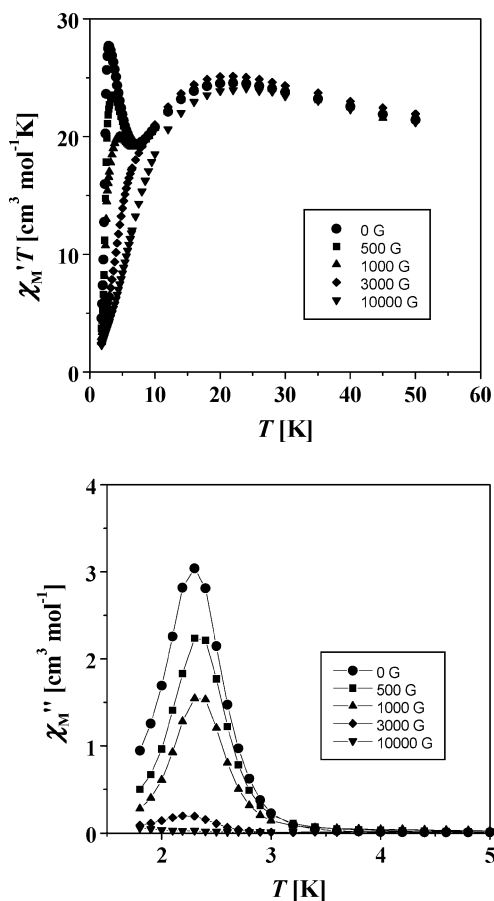


Figure 3. Field dependence of the in-phase and out-of-phase components of the AC magnetic susceptibility for complex **5**. The data were collected at the indicated DC applied magnetic fields and an AC field oscillating at 1 kHz in the 1.8–6.4 K range. The solid line is drawn to guide the eye.

field. It can be seen that there is a peak in the in-phase signal at low field and that this feature disappears as the field is increased. This is what is expected for a 1-D canted antiferromagnet exhibiting metamagnetism.

The slow relaxation of magnetization was examined for a single crystal of **5** with a micro-SQUID magnetometer (Figure 4). In these measurements, data were collected at a scanning rate of 0.002 T/s in the temperature range of 0.04–1.1 K with the applied field parallel to the average easy axis of the one-dimensional polymer. Clearly, the isothermal magnetization of a single crystal of **5** shows a hysteretic response with a significant coercive field and steps at regular magnetic field intervals. This behavior is strongly reminiscent of that observed for an SMM. Each $S = 9$ Mn_4 molecule in the one-dimensional chain exhibits magnetization relaxation as an SMM.² Complex **5** consists of canted antiferromagnetically coupled $S = 9$ Mn_4 molecules in a chain. As can

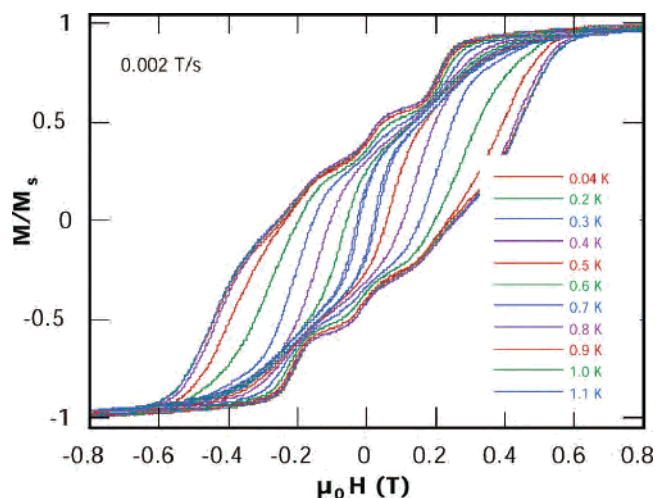


Figure 4. Plot of hysteresis loops for complex **5** with scanning rate 0.002 T/s in the temperature range 0.04–1.1 K.

be seen in Figure 4, the first step in the magnetization hysteresis curve is observed well before the external field is reduced to zero. This shift in the field at which magnetization tunneling occurs is further support for the presence of a weak antiferromagnetic exchange interaction between $S = 9$ $[\text{Mn}_4(\text{hmp})_6]^{4+}$ units. In a recent article,⁶ it was shown that a weak antiferromagnetic interaction ($j'/k_B = -0.05$ K) between two $S = 9/2$ Mn_4 SMMs in a hydrogen-bonded dimer $[\text{Mn}_4]_2$ leads to an “exchange bias” in the magnetic field at which magnetization tunneling occurs. The first magnetization step is not observed at zero field. Additional work is needed to understand the origins of the features evident on the magnetization hysteresis loops shown in Figure 4.

It is important to note that there is considerable interest^{16,17} in magnetization relaxation effects seen in one-dimensional magnetic materials. Caneschi et al.¹⁶ have reported slow magnetization relaxation in a cobalt(II) nitronyl nitroxide chain, dynamics that they attributed to Glauber dynamics expected¹⁸ for a one-dimensional Ising system.

Acknowledgment. This work was supported by the National Science Foundation.

Supporting Information Available: X-ray crystallographic data for complex **5** (CIF, PDF). This material is available free of charge via the Internet at <http://pubs.acs.org>.

IC048212A

(16) Caneschi, A.; Gatteschi, D.; Lalioti, N.; Sangregorio, C.; Sessoli, R.; Venturi, G.; Vindigni, A.; Rettori, A.; Pini, M. G.; Novak, M. A. *Europhys. Lett.* **2002**, *58*, 771–777.

(17) Clerac, R.; Miyasaka, H.; Yamashita, M.; Coulon, C. *J. Am. Chem. Soc.* **2002**, *124*, 12837–12844.

(18) Glauber, R. J. *J. Math. Phys.* **1963**, *4*, 294–307.